

# Grk1b and Grk7a Both Contribute to the Recovery of the Isolated Cone Photoresponse in Larval Zebrafish

Jared D. Chrispell,<sup>1</sup> Enheng Dong,<sup>\*1</sup> Shoji Osawa,<sup>1</sup> Jiandong Liu,<sup>2</sup> D. Joshua Cameron,<sup>3</sup> and Ellen R. Weiss<sup>1,4</sup>

<sup>1</sup>Department of Cell Biology and Physiology, The University of North Carolina at Chapel Hill, Chapel Hill, North Carolina, United States

<sup>2</sup>Department of Pathology and Laboratory Medicine, The University of North Carolina at Chapel Hill, Chapel Hill, North Carolina, United States

<sup>3</sup>College of Optometry, Western University of Health Sciences, Pomona, California, United States

<sup>4</sup>Lineberger Comprehensive Cancer Center, The University of North Carolina at Chapel Hill, Chapel Hill, North Carolina, United States

Correspondence: Ellen R. Weiss, Department of Cell Biology and Physiology, The University of North Carolina at Chapel Hill, 5340B MBRB, Campus Box 7090, Chapel Hill, NC 27599, USA; erweiss@med.unc.edu.

Current affiliation: \*The School of Public Health, Xinxiang Medical University, Xinxiang City, Henan Province, China.

Submitted: March 30, 2018  
Accepted: September 6, 2018

Citation: Chrispell JD, Dong E, Osawa S, Liu J, Cameron DJ, Weiss ER. Grk1b and Grk7a both contribute to the recovery of the isolated cone photoresponse in larval zebrafish. *Invest Ophthalmol Vis Sci.* 2018;59:5116-5124. <https://doi.org/10.1167/iov.18-24455>

**PURPOSE.** To define the functional roles of Grk1 and Grk7 in zebrafish cones in vivo.

**METHODS.** Genome editing was used to generate *grk7a* and *grk1b* knockout zebrafish. Electroretinogram (ERG) analyses of the isolated cone mass receptor potential and the b-wave were performed in dark-adapted zebrafish using a paired flash paradigm to determine recovery of cone photoreceptors and the inner retina after an initial flash. In addition, psychophysical visual response was measured using the optokinetic response (OKR).

**RESULTS.** ERG analysis demonstrated that deletion of either Grk1b or Grk7a in zebrafish larvae resulted in modestly lower rates of recovery of the isolated cone mass receptor potential from an initial flash compared to wildtype larvae. On the other hand, *grk1b*<sup>-/-</sup> and *grk7a*<sup>-/-</sup> larvae exhibited a b-wave recovery that was similar to wildtype larvae. We evaluated the OKR and found that deletion of either Grk1b or Grk7a leads to a small decrease in temporal contrast sensitivity and alterations in visual acuity.

**CONCLUSIONS.** For the first time, we demonstrate that Grk1b and Grk7a both contribute to visual function in larval zebrafish cones. Since the difference between wildtype and each knockout fish is modest, it appears that either GRK is sufficient for adequate cone visual function.

**Keywords:** zebrafish, Grk, photoresponse

Termination of the photoresponse is critical for adaptation to and recovery from light stimuli, and involves a number of molecular components. One essential step is deactivation of the photopigment. The retina-specific members of the G protein-coupled receptor kinase (GRK) family, GRK1 and GRK7, have been implicated in this process via phosphorylation of rhodopsin in rods and the cone opsins in cones.<sup>1-3</sup> GRK1 is expressed in all vertebrate rods, while GRK7 is expressed in cones in all species examined to date except for mice and rats, which express only GRK1 in cones.<sup>3-5</sup> Our own group identified GRK7 in ground squirrel, pig, frog, and human cones. GRK1 and GRK7 are co-expressed in the cones of many vertebrate species, including human, monkey, frog and some fish.<sup>3,6-10</sup> Phosphorylation of cone opsins by GRK7 has also been confirmed in ground squirrel, pig, and fish retinas.<sup>9,11,12</sup>

Comparison of GRK1 and GRK7 activity has been performed in vitro but with inconsistent results.<sup>9,11,13-15</sup> The absence of Grk7 in mice has hampered the understanding of the in vivo contribution of each GRK to the cone photoresponse with implications for understanding cone vision in humans. Therefore, we selected zebrafish (*Danio rerio*) to compare Grk1 and Grk7 function in cones in vivo. As a result of a genome duplication event that occurred in teleosts millions of years ago,

zebrafish possess many gene duplicates (e.g., *grk1a* and *grk1b*, and *grk7a* and *grk7b*).<sup>16</sup> Notwithstanding, zebrafish have a GRK expression profile similar to humans, with rods expressing Grk1a and cones expressing Grk1b and Grk7a.<sup>7,9</sup> Electroretinogram (ERG) analysis can be performed on larvae as early as 3 days post fertilization (dpf), with clear responses obtained at 5 dpf.<sup>17</sup> As little to no scotopic ERG has been reported in wildtype zebrafish larvae younger than 15 dpf,<sup>18</sup> 4-6 dpf larvae are an excellent model for studying the kinetics of the cone photoresponse in vivo. Although Grk7a has been characterized in vivo in zebrafish cones,<sup>7,14</sup> the function of cone-specific Grk1b activity relative to Grk7a has not been addressed.

We examined the contributions of Grk1 and Grk7 to the cone photoresponse at 5 days postfertilization (dpf) in larval zebrafish by modifying the gene structure to eliminate expression of either Grk1b or Grk7a. Using ERG analysis, recovery of the isolated cone mass receptor potential and the b-wave was measured. We also analyzed psychophysical visual function using the optokinetic response (OKR). Our results suggest Grk1b and Grk7a both contribute to signal termination in cones, as deletion of either one had a mild effect on recovery of the cone mass receptor potential. However, deletion of either Grk did not affect recovery of the b-wave, which is



propagated in the inner retina and had only a small effect on the OKR. These results are significantly different from previous studies of Grk7a performed both in vivo and in vitro, demonstrating for the first time a role for Grk1 in cone signal termination.

## METHODS

### Materials

A mouse monoclonal antibody against GRK1 (G8; anti-Grk1) was purchased from Affinity BioReagents (Golden, CO, USA). A rabbit polyclonal antibody against zebrafish Grk7 (anti-Grk7) was generated by 21st Century Biochemicals (Marlboro, MA, USA) against a synthetic peptide corresponding to 521-LFDELDSPNRKESG-535 of zebrafish Grk7a. Anti-FLAG and anti- $\beta$ -actin antibodies were purchased from MilliporeSigma (St. Louis, MO, USA). Secondary antibodies for immunoblot analysis (Alexa Fluor 680 goat anti-rabbit IgG and IRDye800 goat anti-mouse IgG) and immunocytochemistry (Alexa Fluor 488 goat anti-mouse IgG and Alexa Fluor 594 goat anti-rabbit IgG) were purchased from ThermoFisher Scientific (Waltham, MA, USA). All procedures adhered to the ARVO Statement for the Use of Animals of Ophthalmic and Vision Research.

### Immunoblotting

To determine the immunoreactivity of the anti-Grk7 antibody, recombinant FLAG-tagged zebrafish Grk7a and Grk7b were expressed in HEK-293 cells. HEK-293 cells were transfected using FuGENE 6 Transfection Reagent (Promega Corp., Madison, WI, USA) and solubilized by scraping the cells in an SDS buffer (62.5 mM Tris-HCl pH 6.8, 2% SDS [w/v], 20% glycerol [v/v]) containing 100  $\mu$ M NaF. These samples were homogenized briefly with a motorized pestle and the supernatant collected following centrifugation at 10,000g for 10 minutes. Protein concentration was determined using a DC Protein Assay (Bio-Rad, Hercules, CA, USA). Following addition of bromophenol blue and  $\beta$ -mercaptoethanol (final concentrations 0.01% [w/v] and 5% [v/v], respectively), 25  $\mu$ g of the sample protein was analyzed by 10% SDS-PAGE, followed by immunoblot analysis. Nitrocellulose membranes were preincubated in Odyssey Blocking Buffer (Licor Biosciences, Lincoln, NE, USA) and incubated overnight at 4°C with antibodies. Anti-Grk7 and anti-FLAG antibodies were used at a dilution of 1:10,000. AlexaFluor680 and IRDYE800-labeled secondary antibodies were used at 1:15,000. The blots were analyzed using the Odyssey Infrared Imaging System (Licor Biosciences).

To test the anti-Grk7 antibody against endogenous zebrafish protein and determine protein expression levels in knockout zebrafish larvae, 5 dpf larvae or adults were euthanized using a combination of Tricaine (MS-222; Syndel USA, Ferndale, WA, USA) overdose and ice water immersion. Heads from larvae (~20 per sample) or dissected adult retinas (2 per sample) were collected in 50  $\mu$ l of HEPES-Ringer buffer (10 mM HEPES pH 7.5, 120 mM NaCl, 0.5 mM KCl, 0.2 mM CaCl<sub>2</sub>, 0.2 mM MgCl<sub>2</sub>, 0.1 mM EDTA, 10 mM glucose, 1 mM DTT),<sup>19</sup> followed by the addition of 75  $\mu$ l of 2x SDS-Laemmli buffer lacking bromophenol blue and  $\beta$ -mercaptoethanol preheated to 95°C. Samples were homogenized with a motorized pestle and heated for 5 minutes at 95°C. After cooling to room temperature, the samples were sheared with a 25-gauge needle and syringe, heated to 95°C for 2 minutes, and centrifuged at 10,000g for 10 minutes. The supernatant was collected and protein quantified as described above. Bromophenol blue and  $\beta$ -mercaptoethanol were added to 40  $\mu$ g of supernatant from

larval homogenates and 25  $\mu$ g of supernatant from adult fish homogenates. The supernatants were analyzed by 10% SDS-PAGE followed by immunoblot analysis as described above. Anti-Grk7, anti-Grk1, and anti-FLAG antibodies were used at a dilution of 1:10,000, while anti- $\beta$ -actin antibody was used at a 1:5000 dilution, and fluorescently labeled secondary antibodies at a 1:15,000 dilution. Recombinant FLAG-tagged zebrafish Grk1b and Grk7a expressed in HEK-293 cells were purified using an anti-FLAG column and run as quantification standards on the same blots as were samples. Blots were analyzed as described above.

### Immunohistochemistry

Zebrafish larvae at 5 dpf were euthanized, fixed in 4% paraformaldehyde for 30 minutes and cryopreserved through a series of 30-minute incubations using combinations of 5% and 20% sucrose in 0.1 M sodium phosphate buffer, pH 7.2 at room temperature. This series consisted of the following ratios of 5%:20% sucrose: 1:0, 2:1, 1:1, 1:2, and 0:1. Following overnight incubation at 4°C in 20% sucrose, larvae were embedded in low-melting agarose (1.5% [w/v] in 5% sucrose), then embedded in 20% sucrose:OCT (2:1) and flash frozen using 2-methylbutane cooled in liquid N<sub>2</sub>. 20  $\mu$ m sections were cut and co-incubated with anti-Grk7 and anti-Grk1 antibodies at a dilution of 1:1000 and secondary antibodies conjugated to AlexaFluor488 and AlexaFluor594 (1:1500), respectively. Sections were washed in 0.1 M sodium phosphate buffer and mounted in ProLong Gold (Thermo Fisher Scientific). Images were collected by confocal microscopy using a Zeiss 880 microscope (Zeiss, Oberkochen, Germany) and analyzed using Zen Blue software (Zeiss).

### TALEN Construction

Sequences from exons 1 of both *grk1b* and *grk7a* were scanned for potential TALEN target sites using the TALEN Targeter program (<https://tale-nt.cac.cornell.edu/>, provided in the public domain by Cornell University, Ithaca, NY, USA). Off-target sites were avoided using the Targeter against the Zv9 Zebrafish Genome Assembly and by in-house BLAST to remove Left and Right TAL-binding sites in close proximity.

Grk7aEx1\_TALEN\_Left: CTGTCTCTGCCCAAGCCGG;  
Grk7aEx1\_TALEN\_Right: TCAGGACGAGTCTGGACAAGG;  
Grk1bEx1\_TALEN\_Left: TAGCAAGCTCAACCTGCCACAC;  
Grk1bEx1\_TALEN\_Right: AAATGAAGACTATAGTGGATA

Left and Right target sequences for each gene were cloned into pCSTAL3DD and pCS2TAL3RR, respectively, utilizing Golden Gate cloning. mRNA was synthesized from linearized vectors using the mMMESSAGE mMACHINE SP6 Kit (Thermo Fisher Scientific). One-cell zebrafish embryos were injected with 2.3 nl of a mixture consisting of 2  $\mu$ l of Left TAL mRNA (200 ng/ $\mu$ l), 2  $\mu$ l of Right TAL mRNA (200 ng/ $\mu$ l), 1  $\mu$ l of phenol red, and 5  $\mu$ l of distilled deionized water (ddH<sub>2</sub>O).

### Screening of Mutants

Mutants were identified using high resolution melting analysis (HRMA) and DNA sequencing. Genomic DNA was purified by proteinase K digestion of fin clippings or whole euthanized 3 dpf larvae, followed by ethanol precipitation. DNA was resuspended in 100  $\mu$ l of ddH<sub>2</sub>O. For HRMA, primers were designed to flank the target and produce an amplicon between 60 and 100 bp. Each reaction mixture consisted of 9  $\mu$ l of primer mix (0.7  $\mu$ M of each primer), 10  $\mu$ l of SYBRGreen PCR Master Mix (Life Technologies, Thermo Fisher Scientific), and 1  $\mu$ l of genomic DNA. The PCR reaction and melt analysis were performed using a Viia 7 Real-Time PCR system with the

following protocol: 50°C for 2 minutes; 95°C for 10 minutes; 95°C for 10 seconds; 60°C for 30 seconds, repeat the last two steps 40 times; 95°C for 15 seconds; 55°C for 15 seconds; 95°C for 15 seconds. Viia 7 software was used to perform analysis of aligned fluorescence. Founders were identified by screening F1 progeny resulting from crossing F0 fish to wildtype fish. Fin clips of F1 heterozygotes were sequenced to identify frame-shifted nonsense mutants, and matching heterozygotes were crossed to generate homozygous knockout zebrafish. F2 knockouts were confirmed by sequencing and immunoassay.

### Electroretinogram (ERG) Analysis

ERG analysis was performed as described previously.<sup>20,21</sup> Briefly, 5 dpf larvae were dark-adapted overnight prior to analysis. Fish were incubated for 5 minutes under indirect dim white light (<1 lux) in system H<sub>2</sub>O with 2-amino-4-phosphonobutyric acid (APB; 500 μM; DL-AP4 #0101; Bio-Techne/Tocris, Minneapolis, MN, USA) to allow measurement of the isolated cone mass receptor potential. Larvae were anesthetized with 0.02% Tricaine and positioned under low light (275 lux for ≤1 min) on a damp sponge saturated with oxygenated Goldfish Ringer's buffer.<sup>22</sup> The microelectrode (consisting of an AgCl wire in a glass capillary with a 10 μm tip filled with Goldfish Ringer's buffer) was positioned on the cornea. An AgCl pellet underneath the sponge served as a reference electrode. Once positioned, larvae were allowed to dark-adapt for 5 minutes. Recordings were obtained using a Diagnosys Espion E<sup>2</sup> system and Colordome (Diagnosys LLC, Lowell, MA, USA) with a modified stage. The sensitivity of the cone mass receptor potential was determined using a single flash paradigm consisting of 20-ms flashes of white LED light with intensities of 1, 5, 10, 20, 50, 100, 500, 1000, 2000, and 5000 cd/m<sup>2</sup>. Recovery to successive stimuli was determined using a dual flash paradigm that utilized two 20-ms flashes of white LED light with an intensity of 1000 cd/m<sup>2</sup> separated by variable interstimulus intervals (ISIs) of darkness.

### Optokinetic Response (OKR)

Several 5–6 dpf larvae were anesthetized with 0.02% Tricaine and immobilized in 3% methylcellulose. They were positioned in the center of a 75-mm drum on average 31.5 mm from the edge. The larvae revive from anesthesia within a few minutes and random eye movements are observed. To measure visual acuity, a base grating of 0.03 cycles per degree (cpd) is placed into the rotating drum and the computer controls engaged to begin rotation (8–16 rpm) and video capture. Once an initial OKR was elicited by the base grating, the rotation was paused and the base grating replaced with a smaller grating to measure higher spatial frequency. This process was repeated using increasingly smaller gratings until an OKR could no longer be elicited. Loss of the OKR was verified by retesting with the gratings following a modified staircase approach. The maximum visual acuity was obtained by calculating the cpd:

$$\frac{1}{2 \tan^{-1} \left( \frac{b}{2a} \right)},$$

where  $a$  is the distance from the eye to the grating and  $b$  is the length of one cycle of the smallest grating at which OKR was observed.<sup>23</sup>

Temporal contrast sensitivity for 5–6 dpf larvae was measured by the optokinetic gain (eye velocity/grating velocity) as a function of temporal frequency. Movement direction of the grating was varied using a computer software program. The pattern velocity of a sine grating was varied

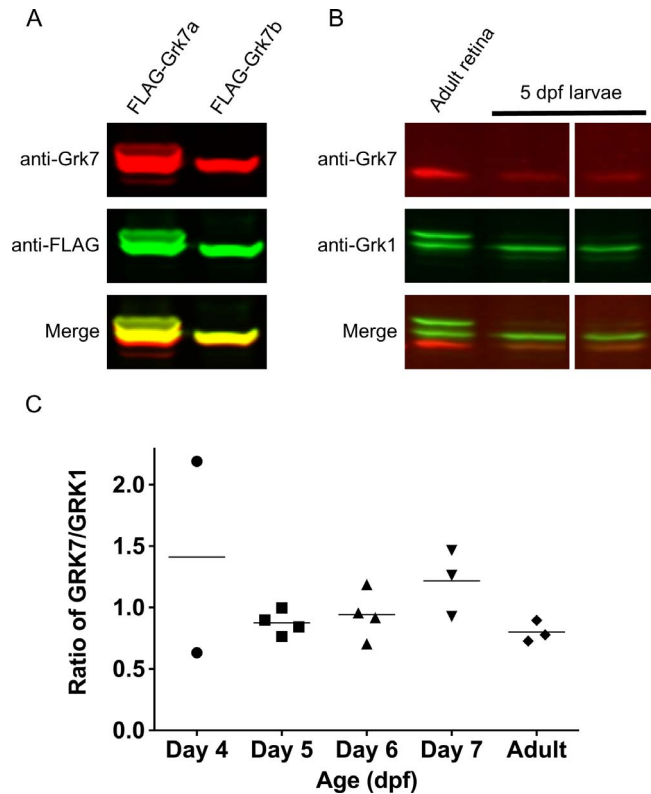


**FIGURE 1.** Relative protein expression of Grk homologs in zebrafish cones using a novel zebrafish-specific anti-Grk7 antibody. (A) Immunodetection of 25 μg each of recombinant FLAG-tagged Grk7a and Grk7b prepared from HEK293 cells as described in “Methods.” For immunodetection, the immunoblot was incubated with anti-Grk7 (*red*) and anti-FLAG (*green*) antibodies at dilutions of 1:10,000 followed by incubation with secondary antibodies at a dilution of 1:15,000. (B) Immunodetection of endogenous Grk proteins in isolated retinal homogenates of adult zebrafish and heads of 5 dpf larvae. 40 μg of protein was loaded in each lane and the immunoblot was probed using a 1:10,000 dilution of the anti-Grk7 (*red*) and anti-Grk1 (*green*) antibodies followed by incubation with a 1:15,000 dilution of the secondary antibodies. (C) Ratio of Grk7 to Grk1 protein expression during zebrafish development. Samples were prepared, immunoblotting performed and quantification performed using Flag-tagged Grk1 and Grk7 as described in “Methods.”

while keeping all other parameters constant. Larvae were adapted for 2 minutes to a background of 1100 lux. Then a temporal frequency pattern (0.03 cycles/deg) with a velocity of 7.4 deg/s was presented, and optokinetic gain was measured for at least 2 periods. Spatial frequency was maintained at 0.03 cycles/deg, and gain was determined for 7.4, 10.8, 21.6, 25.2 and 37.8 deg/s.<sup>7</sup>

### Statistical Analyses

For single flash ERG experiments, normalized peak amplitude responses were fitted using the Naka Rushton function with GraphPad Prism (La Jolla, CA, USA).<sup>24</sup> For dual flash ERGs and temporal contrast OKR, we fit linear mixed models of covariance to compare response recovery between genotypes across repeated ISI levels. Models included random fish effects to account for within-fish correlations. These analyses were performed using JMP (SAS, Cary, NC, USA). For OKR measurements of visual acuity, responses in cycles/degree (cpd) were analyzed by 1-way ANOVA and pairwise comparisons were performed using the Bonferroni post hoc test in

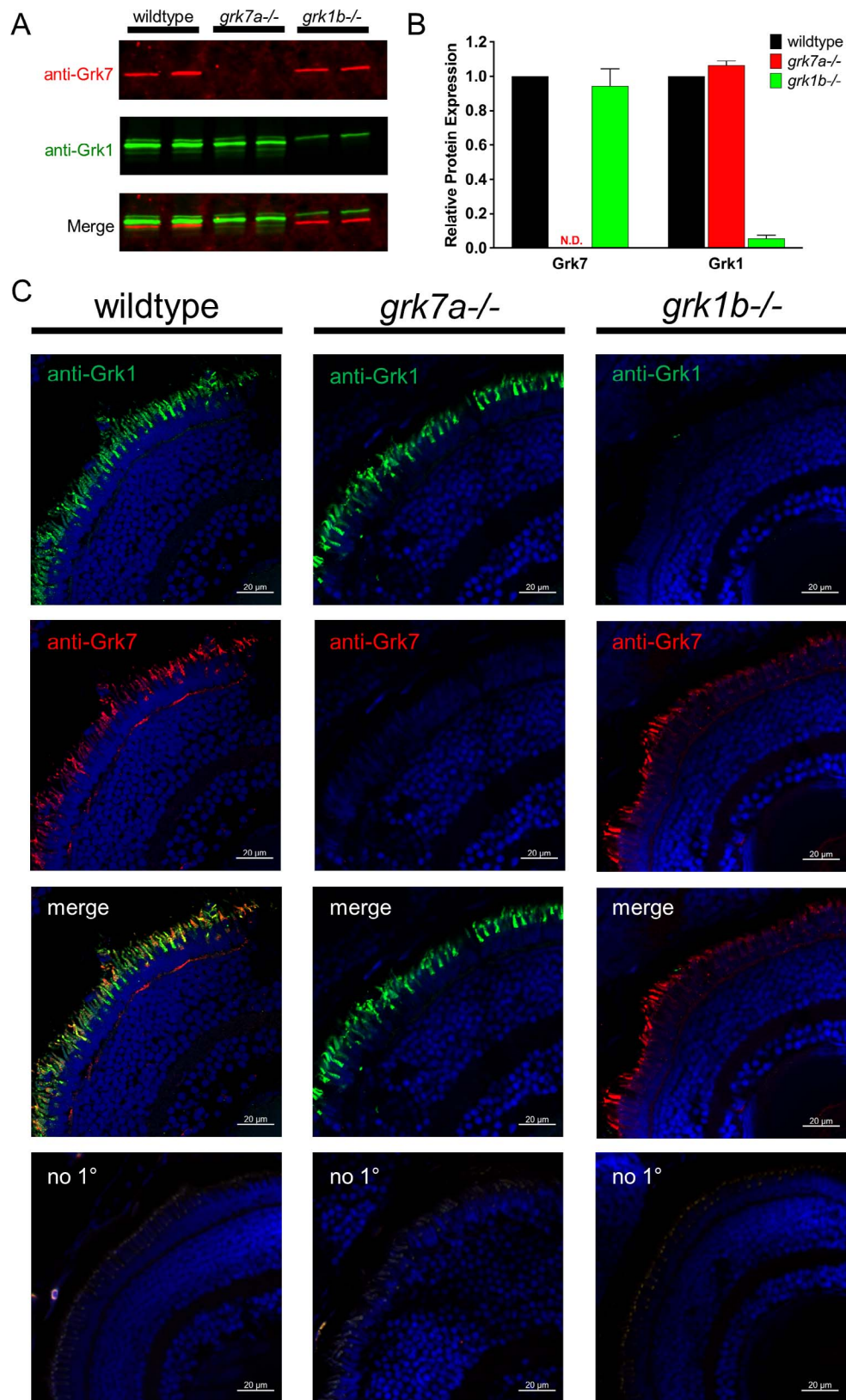


**FIGURE 2.** Detection of Grk1b and Grk7a in knockout larvae. **(A)** Immunoblot analysis of tissue homogenates isolated from heads of light-adapted wildtype, *grk7a*<sup>-/-</sup>, and *grk1b*<sup>-/-</sup> larvae at 5 dpf. 40  $\mu$ g of each sample were loaded per lane. Immunoblots were probed with antibodies against Grk7 (red) and Grk1 (green) followed by incubation with secondary antibodies as described in “Methods.” **(B)** Relative expression of total Grk1 and Grk7 in knockout lines compared to wildtype larvae at 5 dpf was quantified from the data in **(A)**. All samples were normalized to  $\beta$ -actin immunoreactivity. Bars represent the range of duplicate samples. N.D., none detected. **(C)** Immunocytochemical analysis of knockout larvae at 5 dpf. Light-adapted larvae were fixed, cryoembedded, and sectioned as described in “Methods.” Sections were probed with anti-Grk7 (red) and anti-Grk1 (green) at a dilution of 1:1000, followed by incubation in secondary antibodies conjugated to AlexaFluor488 and AlexaFluor594, respectively at a dilution of 1:1500.

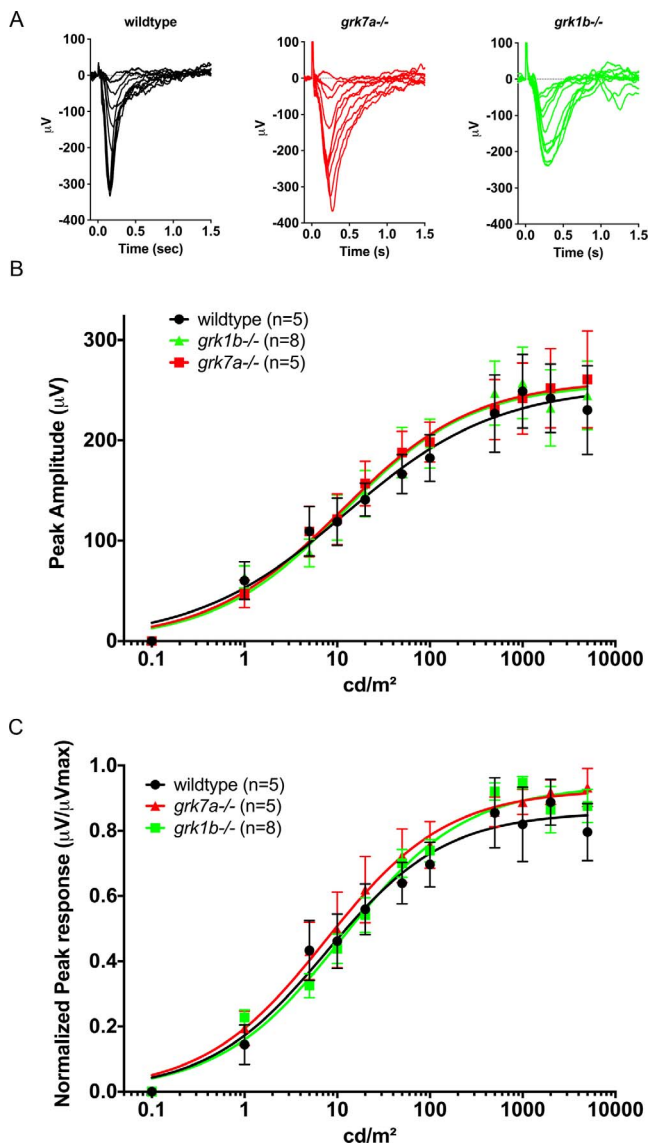


**FIGURE 3.** Electrophysiological light responses and normalized sensitivity of *grk1b* and *grk7a* knockout larvae. (A) Representative ERG traces of isolated cone-mass receptor potentials in APB-treated larvae at 5 dpf. Responses were recorded under dark-adapted conditions to 20-ms flashes of light of increasing intensities equal to 0.1, 1, 10, 25, 50, 125, 250, 500, 1250, 2500, and 5000  $\text{cd}/\text{m}^2$ . The fast initial positive deflection can be attributed to a photovoltaic effect with the recording microelectrode. (B) Peak amplitude responses of 5 dpf larvae fit using the Naka-Rushton function. (C) Mean-normalized peak response amplitudes of 5 dpf larvae fit using the Naka-Rushton function. Error bars represent SEM.

GraphPad Prism. For all analyses, a *P* value of 0.05 was considered significant.

## RESULTS

### Grk1 and Grk7 Expression Levels Are Similar in Larval Zebrafish

The commercially available GRK1 antibody (G8) has been shown to recognize GRK1 in a number of species, including Grk1a and Grk1b in zebrafish.<sup>4,5,9,25–27</sup> We generated a rabbit polyclonal antibody that recognizes both paralogs of zebrafish

Grk7 (Grk7a and Grk7b). HEK-293 cells expressing recombinant FLAG-tagged Grk7a or Grk7b were harvested and subjected to immunoblotting with anti-Grk7 and anti-FLAG antibodies (Fig. 1A). Detection of both recombinant Grk7 paralogs by western blot analysis using anti-Grk7 was robust. When anti-Grk7 immunoreactivity was merged with that of the anti-FLAG antibody, complete overlap of signal is observed. No anti-Grk7 immunoreactivity was observed against nontransfected lysates or HEK-293 cells transfected with recombinant zebrafish Grk1 paralogs (Supplementary Fig. S1A). These observations demonstrate the reliability of our anti-Grk7 antibody for detecting Grk7 levels in zebrafish. Using purified FLAG-tagged recombinant zebrafish Grk7a and Grk1b as quantification standards (Supplementary Fig. S1B), the ratio of Grk7 to Grk1 immunoreactivity in 5 dpf larvae is 0.8 and comparable to the ratio observed in adult zebrafish retinas (Fig. 1B, 1C). Neither Grk1 nor Grk7 protein expression was detected between 1–3 dpf (data not shown), while the variation in expression ratios observed at 4 dpf may be due to variability of the developmental stage (Fig. 1C).

### Characterization of *grk7a* and *grk1b* Knockout Zebrafish

To understand the relative importance of the retina-specific GRKs to the mechanism of cone adaptation and recovery, we eliminated expression of the cone-specific paralogs Grk7a and Grk1b as described in “Methods.” DNA sequencing shows a 7-bp deletion/6-bp insertion within exon 1 of *grk7a* and a 4-bp deletion in exon 1 of *grk1b*. These mutations result in massively truncated forms of each Grk protein, at 53 amino acids for Grk7a and 48 amino acids for Grk1b (data not shown). To confirm that these genomic alterations translate to changes at the protein level, immunoblot assays were performed. Analysis of *grk7a*<sup>-/-</sup> larvae at 5 dpf show undetectable levels of Grk7 compared to wildtype (Fig. 2A, 2B). In *grk1b*<sup>-/-</sup> larvae at 5 dpf, Grk1 expression levels are reduced by 95% of that observed in wildtype larvae (Fig. 2A, 2B). As the Grk1 antibody does not distinguish between the Grk1a and Grk1b paralogs, the remaining Grk1 immunoreactivity may be early expression of minute amounts of Grk1a in immature rod photoreceptors. However, immunocytochemical analysis of *grk1b*<sup>-/-</sup> larvae display no anti-Grk1 staining and confirms effective deletion of Grk1b compared to wildtype (Fig. 2C, last column). Immunocytochemical analysis also confirms knockout of Grk7 expression in *grk7a*<sup>-/-</sup> larvae, with no anti-Grk7 immunoreactivity compared to wildtype (Fig. 2C, middle column). Wildtype larvae double-labeled with anti-Grk1 and anti-Grk7 antibodies (Fig. 2C, first column) display immunocytochemical colocalization, which can be attributed to cone photoreceptors based on previous reports of Grk7a localization in larval cones.<sup>7</sup> Despite the respective Grk deficiencies on a proteomic level in the larval retina, brightfield images of whole *grk7a*<sup>-/-</sup> and *grk1b*<sup>-/-</sup> larvae appear indistinguishable from wildtype larvae (Supplementary Fig. S2).

### Normalized Photopic Sensitivity Is Unchanged in Grk7a- and Grk1b-Deficient Larvae

To compare cone function between wildtype, *grk7a*<sup>-/-</sup>, and *grk1b*<sup>-/-</sup> larvae, ERG analysis was performed. At 5 dpf, the ERG response of the zebrafish is elicited only by photopic stimuli since nascent rods are not functional at this age.<sup>18,28,29</sup> The photopic response is generally characterized by a very small a-wave (cone photoreceptor contribution) and a robust b-wave (inner retina contribution). To isolate the cone mass receptor potential from other elements of the ERG response, we incubated whole larvae for 5 minutes in the metabotropic

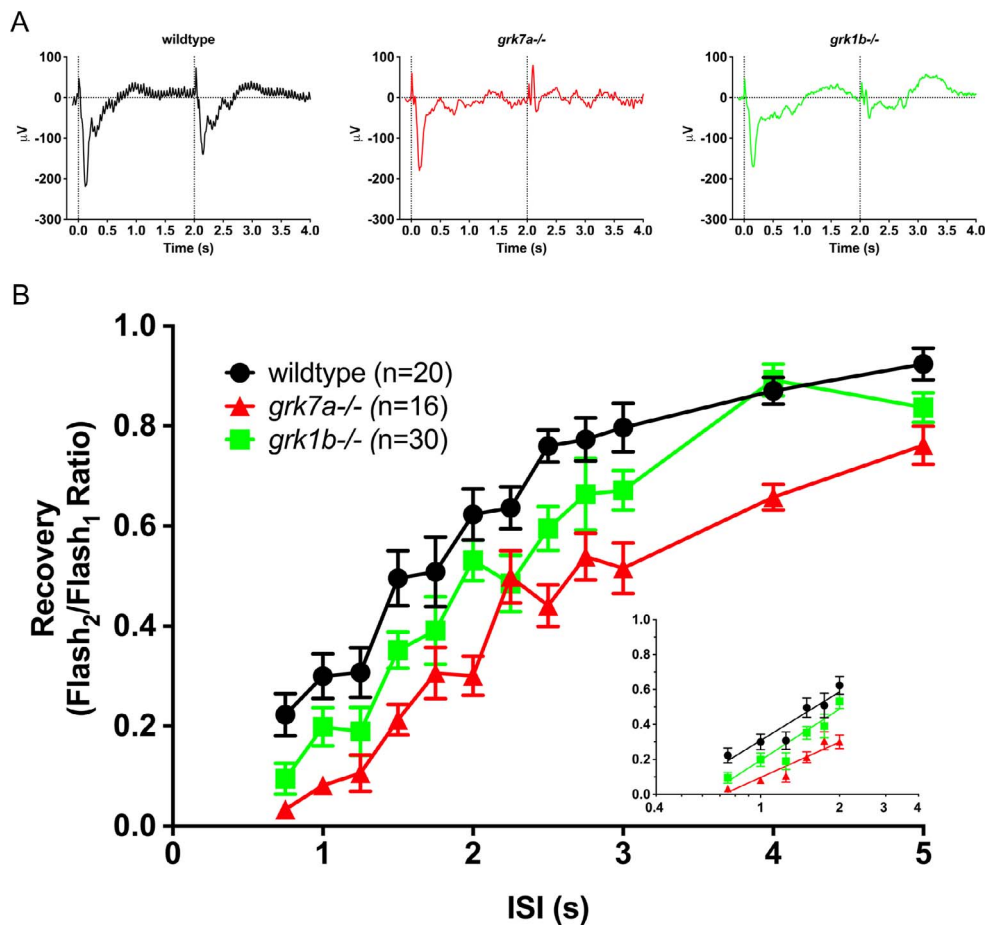


**FIGURE 4.** Recovery of the isolated cone-mass receptor potential to successive stimuli. (A) Representative ERG waveforms of APB-treated, dark-adapted larvae subjected to successive stimuli using a dual flash paradigm of a 20-ms flash of saturating white light ( $1000 \text{ cd/m}^2$ ) with an interstimulus interval (ISI) of 2 s. Vertical black dotted lines indicate time of stimulus. (B) Data are plotted as the ratio of the maximum isolated cone mass receptor potential response of the second stimulus to that of the initial stimulus for ISIs ranging from 0.75 s to 5 s. A linear mixed model analysis of covariance found a significant effect of genotype when compared to wildtype for *grk1b*<sup>-/-</sup> ( $F_{[1,49]} = 6.5$ ;  $P = 0.0142$ ) and *grk7a*<sup>-/-</sup> ( $F_{[1,33]} = 36.6$ ;  $P < 0.001$ ). Inset, regression to the logarithmic linear part of the recovery kinetics.<sup>7</sup> Error bars represent SEM.

glutamate receptor 6 (mGluR6) agonist APB prior to recording. Responses were recorded across an intact eye to single 20-ms flashes of white light of intensities from 0.1 to  $5000 \text{ cd/m}^2$  (Fig. 3A, representative traces). Peak amplitudes were fit using the Naka-Rushton equation (Fig. 3B).<sup>24</sup> To compare cone sensitivity in wildtype and genetically modified fish, responses were normalized ( $\mu\text{V}/\mu\text{V}_{\text{Max}}$ ) and also fit with the Naka-Rushton equation (Fig. 3C). No significant differences in peak amplitudes or normalized sensitivity were observed between *grk7a*<sup>-/-</sup>, *grk1b*<sup>-/-</sup>, and wildtype larvae.

#### Recovery of Cone Mass Receptor Potential Is Decreased in *grk1b*<sup>-/-</sup> and *grk7a*<sup>-/-</sup> Larvae

To determine if the deletion of endogenous Grk7a or Grk1b at 5 dpf affects the cone response recovery, we analyzed ERG responses to successive stimuli with variable interstimulus intervals (ISIs; Fig. 4). APB-treated larvae were subjected to a conditioning flash of saturating white light ( $1000 \text{ cd/m}^2$ , 20 ms), followed by a probe flash of the same intensity at varying intervals. Recovery was measured as the ratio of the cone mass receptor potential of the probe flash to the initial conditioning flash. Sample recovery waveforms using an ISI of 2 seconds are shown in Figure 4A. A time course of the cone

mass receptor potential recovery shows a moderate but statistically significant delayed response for both *grk1b*<sup>-/-</sup> and *grk7a*<sup>-/-</sup> larvae compared to wildtype larvae (Fig. 4B). A logarithmic linear regression of the non-saturating portion of the response shows a recovery half-life of 1.7 seconds for wildtype larvae, versus 2.3 and 3.0 seconds for *grk1b*<sup>-/-</sup> and *grk7a*<sup>-/-</sup> larvae, respectively (Fig. 4B, inset).

#### *grk1b*<sup>-/-</sup> and *grk7a*<sup>-/-</sup> Larvae Exhibit Recovery of b-Wave Response Equivalent to Wildtype

To evaluate the influence of the decreased recovery observed in cones on downstream signaling, we performed ERG analysis on wildtype, *grk1b*<sup>-/-</sup>, and *grk7a*<sup>-/-</sup> larvae at 5 dpf in the absence of APB treatment using the same dual flash paradigm. This allowed us to analyze the b-wave generated by the propagation of the visual signal through the retinal cells postsynaptic to the photoreceptors, which dominates the native zebrafish larval ERG waveform (reviewed in Ref. 30).<sup>20,51</sup> Sample recovery waveforms using an ISI of 2 seconds are shown in Figure 5A. Unlike the cone mass receptor potential, the recovery of the b-wave in *grk1b*<sup>-/-</sup> and *grk7a*<sup>-/-</sup> larvae was not statistically different from recovery in wildtype larvae (Fig. 5B).

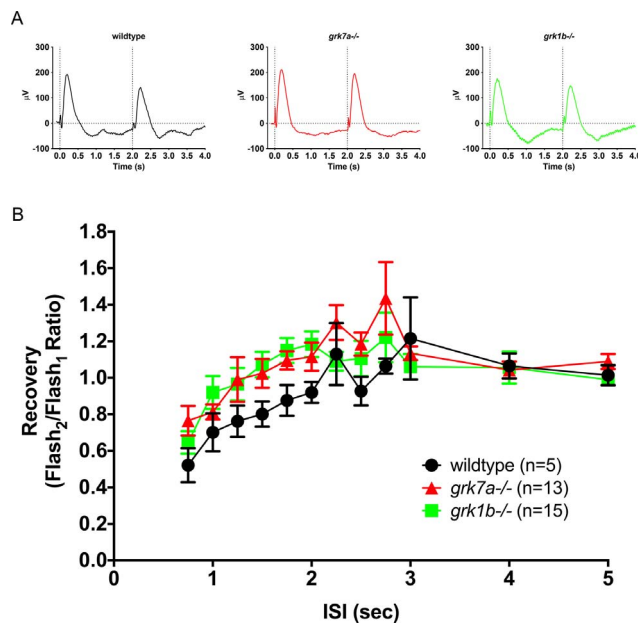


**FIGURE 5.** Recovery of the native ERG b-wave to successive stimuli in *grk* knockout zebrafish larvae. (A) Representative ERG waveforms of untreated, dark-adapted larvae subjected to successive stimuli using a dual flash paradigm of a 20-ms flash of saturating white light (1000 cd/m<sup>2</sup>) with an interstimulus interval (ISI) of 2 s. Vertical black dotted lines indicate the time of stimulus. (B) Data are plotted as the ratio of the maximum b-wave response amplitude of the second stimulus to that of the initial stimulus for ISIs ranging from 0.75 s to 5 s. A linear mixed model analysis of covariance found no significant effect of genotype when compared to wildtype for *grk1b*<sup>-/-</sup> ( $F_{[1,14]} = 1.2$ ;  $P = 0.2879$ ) or *grk7a*<sup>-/-</sup> larvae ( $F_{[1,17]} = 3.3$ ;  $P = 0.0889$ ). Error bars represent SEM.

### Deletion of Grk7a or Grk1b Causes Mild Visual Dysfunction in Larval Zebrafish

To determine if psychophysical visual function was affected by the absence of Grk7a or Grk1b, the optokinetic response (OKR) of the larvae was measured. OKR analysis is a behavioral assay characterized by a combination of smooth pursuit and rapid saccade eye movements in response to whole field movements in the surroundings. The OKR can be used to determine contrast sensitivity in zebrafish larvae by measuring the velocity of the eye movements to stimuli of increasing velocity. The optokinetic gain (eye velocity/stimulus velocity) is a function of stimulus contrast and is indicative of temporal contrast sensitivity.<sup>32</sup> A very small but statistically significant decrease was observed for both *grk7a*<sup>-/-</sup> and *grk1b*<sup>-/-</sup> larvae at 6 dpf compared to wildtype (Fig. 6A). By altering the spatial frequency of the stimulus, we were also able to measure the visual acuity of the larvae (Fig. 6B). Compared to wildtype larvae, visual acuity in *grk7a*<sup>-/-</sup> larvae was found to be approximately 17% higher. Conversely, *grk1b*<sup>-/-</sup> larvae exhibited a 16% decrease in visual acuity compared to wildtype larvae.

### DISCUSSION

The zebrafish larva is an established model for studying cone sensitivity and recovery with the same retinal GRK expression profile as humans. The zebrafish retina expresses a Grk1 paralog in both rods and cones (Grk1a and Grk1b, respectively) and a Grk7 paralog (Grk7a) in cones.<sup>9,33,34</sup> The retina

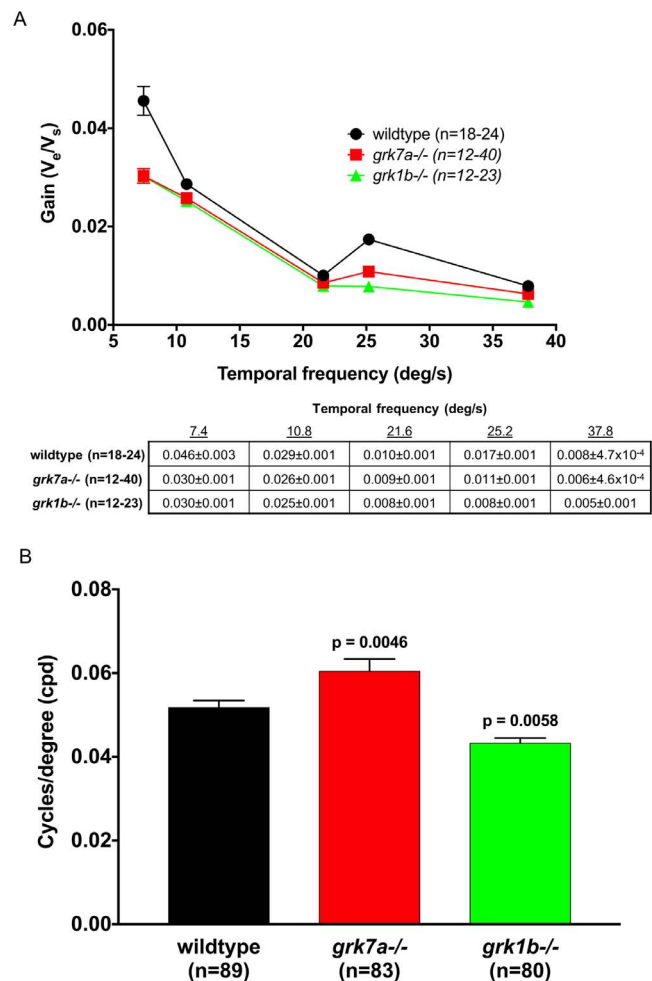


**FIGURE 6.** Temporal contrast sensitivity and visual acuity of *grk1b* and *grk7a* knockout larvae. Optokinetic response measurements of larval knockout zebrafish at 6 dpf. (A) Optokinetic gain as function of temporal frequency of a sinewave grating. A linear mixed model analysis of covariance found a significant effect of genotype when compared to wildtype for *grk1b*<sup>-/-</sup> ( $F_{[1,209]} = 32.9$ ;  $P < 0.001$ ) and *grk7a*<sup>-/-</sup> ( $F_{[1,193]} = 21.4$ ;  $P < 0.001$ ) larvae. The accompanying table shows all means and standard errors from the graph. (B) Visual acuity measured in cycles/degree (cpd). P-values were obtained using the Bonferroni post hoc test following 1-way ANOVA. Error bars represent SEM.

develops rapidly, with cone maturation allowing for behavioral and electrophysiological analyses as early as 4 dpf.<sup>20,31</sup> While nascent rods are present in the developing zebrafish retina, their contribution to visual function is largely undetectable prior to 15 dpf.<sup>18,29</sup> The larval zebrafish can thus be considered functionally an “all cone” retina at 5–6 dpf.

We show by ERG that when either cone-specific Grk is eliminated from zebrafish larvae, recovery of the cone mass receptor potential is modestly delayed compared to wildtype (Fig. 4). The *grk7a*<sup>-/-</sup> larvae demonstrated slightly slower recovery than the *grk1b*<sup>-/-</sup>, although full recovery was ultimately achieved in both mutants. We also measured recovery of the b-wave for all three fish lines to determine how effectively the photoresponse is transmitted from cones to the inner retina, primarily the ON bipolar cells. The *grk1b*<sup>-/-</sup> and *grk7a*<sup>-/-</sup> larvae were similar to wildtype larvae, suggesting that these Grks functionally substitute for each other. Finally, we also evaluated the OKR in these fish, which

demonstrated mildly affected yet operable contrast sensitivity and visual acuity.

In a previous study, where Grk7a was suppressed using morpholinos, the b-wave measured in zebrafish larvae demonstrated lower recovery, whereas we did not observe this in our studies.<sup>7</sup> Deletion of either Grk1b or Grk7a also resulted in a smaller decrease in OKR in our studies than reported by Rinner et al. for Grk7a knockdown.<sup>7</sup> Our data indicate that neither Grk1 nor Grk7 deletion translates to severe visual deficiency as measured by OKR. These contrasting results may be due to side effects of morpholino knockdown, which have been reported to give variable results.<sup>35</sup> There may also be developmental differences in gene expression between suppression via morpholinos versus genetic deletion.

Previous reports comparing Grk1 and Grk7 in vitro have measured the levels and activities of the two kinases in zebrafish and carp. In zebrafish, the Grk7/Grk1 ratio was reported to be 1.6,<sup>9</sup> which is only 2-fold different than our result (0.8) in Figure 1C. Surprisingly, in Wada et al.,<sup>9</sup> the  $V_{max}$  for Grk7 was 32-fold higher than for Grk1. In carp, a 10-fold higher level of Grk7 expression compared to Grk1 was observed and phosphorylation activity was 10 times higher in cone membranes than rod membranes, implying that Grk7 has the highest catalytic activity of any GRK family member and implicating this kinase in accelerated turnoff in cones.<sup>11,36</sup> Although our ERG measurements of the isolated cone mass receptor potential suggest that Grk7 makes a more significant contribution to the termination and recovery of the photoresponse in zebrafish cones, this difference is not as profound as would be expected based on the studies described above. Importantly, our work demonstrates that the effect of deletion of a single Grk is not sufficient to cause detectable changes in b-wave recovery, and changes in the OKR are modest.

Another interesting observation from our study was that knockout of either *grk1b* or *grk7a* was associated with a small change in visual acuity as measured by OKR. A number of cone dystrophies are characterized by a loss in patient visual acuity (reviewed in Ref. 37), but such a loss has not been observed in patients with inactivating GRK1 mutations. Despite this, the 16% decrease in visual acuity observed in *grk1b*<sup>-/-</sup> larvae may be an indicator of mild cone dysfunction, while *grk7a*<sup>-/-</sup> larvae exhibited a 17% increase in visual acuity. It has been observed that the cone mosaic in the developing larval zebrafish is relatively disorganized compared to the adult, and each of the 4 cone opsins have their own dedicated precursors.<sup>38,39</sup> It is possible that the knockout of either *grk7a* or *grk1b* has an impact on the formation of the functional cone mosaic and, therefore, the spatial resolution. In the future, we plan to examine the larval fish at various ages 4–7 dpf looking at cone organization and color-specific cone function as well as any developmental changes in the retina between the two groups. These future studies will also include analysis of knockout larval emmetropization and ocular morphology.

The human retina expresses GRK1 in both rods and cones and GRK7 in cones similar to zebrafish.<sup>3,4,40,41</sup> Deficiencies in GRKs are associated with retinal pathologies, providing insight into their role in visual function. An inactivating mutation in GRK1 is found in some patients with Oguchi disease, a condition characterized by stationary night blindness, associated with a defect in rod adaptation.<sup>42,43</sup> Mice (which express GRK1 in rods and cones) also demonstrate impaired rhodopsin inactivation kinetics in *Grk1*<sup>-/-</sup> mice.<sup>43–45</sup> However, *Grk1*<sup>-/-</sup> mice exhibit greater impaired cone recovery than human patients,<sup>45</sup> consistent with the presence of GRK7 in human cones and its absence in mice. In another example, patients with Enhanced S-Cone

Syndrome (ESCS) display a retina largely lacking rods but with an abundance of S-cones.<sup>46,47</sup> These S-cones lack both GRK1 and GRK7, and the isolated S-cone recovery response is highly delayed compared to normal S-cones. In contrast, the L/M-cones in ESCS patients lack GRK7 and demonstrate a small delay in recovery compared to normal L/M-cones. Recovery is only moderately faster than L/M-cones in Oguchi patients, which lack GRK1.<sup>48</sup> These results are consistent with our observations in zebrafish, suggesting that GRK1 and GRK7 make similar contributions to cone recovery.

The novel results of our studies underscore the participation of either cone-specific Grk1b and Grk7a in recovery of the larval zebrafish cone photoresponse and ultimately to vision itself. They also corroborate observations seen in disease models of GRK deletion and dysfunction. In contrast to other studies in model organisms, both in vivo and in vitro, our experiments using targeted loss-of-function analysis in zebrafish suggest that the in vivo contributions of each GRK to cone recovery is similar and relevant to human cone vision.

### Acknowledgments

The authors thank Paul Stewart, PhD, for advice on the statistical analysis and Tatiana Rebrik, PhD, for help with establishing the zebrafish ERG technique and data interpretation. We would also like to thank Michelle Altemara, MS, and the Zebrafish Aquaculture Core Facility at The University of North Carolina at Chapel Hill for maintenance of zebrafish stocks.

Supported by National Institutes of Health Grants NEI R01EY12224 (ERW), 1F32EY022279 (JDC), R00 HL109079 (JL), and the Duke Core Grant for Vision Research P30EY05722.

Disclosure: **J.D. Chrisspell**, None; **E. Dong**, None; **S. Osawa**, None; **J. Liu**, None; **D.J. Cameron**, None; **E.R. Weiss**, None

### References

- Maeda T, Imanishi Y, Palczewski K. Rhodopsin phosphorylation: 30 years later. *Prog Retin Eye Res.* 2003;22:417–434.
- Metayé T, Gibelin H, Perdrisot R, Kraimps JL. Pathophysiological roles of G-protein-coupled receptor kinases. *Cell Signal.* 2005;17:917–928.
- Shi ER, Ducceschi MH, Horner TJ, Li A, Craft CM, Osawa S. Species-specific differences in expression of G-protein-coupled receptor kinase (GRK) 7 and GRK1 in mammalian cone photoreceptor cells: implications for cone cell phototransduction. *J Neurosci.* 2001;21:9175–9184.
- Zhao X, Huang J, Khani SC, Palczewski K. Molecular forms of human rhodopsin kinase (GRK1). *J Biol Chem.* 1998;273:5124–5131.
- Zhao X, Yokoyama K, Whitten ME, Huang J, Gelb MH, Palczewski K. A novel form of rhodopsin kinase from chicken retina and pineal gland. *FEBS Lett.* 1999;454:115–121.
- Hisatomi O, Matsuda S, Satoh T, Kotaka S, Imanishi Y, Tokunaga F. A novel subtype of G-protein-coupled receptor kinase, GRK7, in teleost cone photoreceptors. *FEBS Lett.* 1998;424:159–164.
- Rinner O, Makhankov YV, Biehlmair O, Neuhauss SC. Knockdown of cone-specific kinase GRK7 in larval zebrafish leads to impaired cone response recovery and delayed dark adaptation. *Neuron.* 2005;47:231–242.
- Shimauchi-Matsukawa Y, Aman Y, Tachibanaki S, Kawamura S. Isolation and characterization of visual pigment kinase-related genes in carp retina: polyphyly in GRK1 subtypes, GRK1A and 1B. *Mol Vis.* 2005;11:1220–1228.
- Wada Y, Sugiyama J, Okano T, Fukada Y. GRK1 and GRK7: unique cellular distribution and widely different activities of opsin phosphorylation in the zebrafish rods and cones. *J Neurochem.* 2006;98:824–837.

10. Weiss ER, Raman D, Shirakawa S, et al. The cloning of GRK7, a candidate cone opsin kinase, from cone- and rod-dominant mammalian retinas. *Mol Vis*. 1998;4:27.
11. Tachibanaki S, Arinobu D, Shimauchi-Matsukawa Y, Tsushima S, Kawamura S. Highly effective phosphorylation by G protein-coupled receptor kinase 7 of light-activated visual pigment in cones. *Proc Natl Acad Sci U S A*. 2005;102:9329-9334.
12. Liu P, Osawa S, Weiss ER. M opsin phosphorylation in intact mammalian retinas. *J Neurochem*. 2005;93:135-144.
13. Horner TJ, Osawa S, Schaller MD, Weiss ER. Phosphorylation of GRK1 and GRK7 by cAMP-dependent protein kinase attenuates their enzymatic activities. *J Biol Chem*. 2005;280:28241-28250.
14. Vogalis F, Shiraki T, Kojima D, et al. Ectopic expression of cone-specific G-protein-coupled receptor kinase GRK7 in zebrafish rods leads to lower photosensitivity and altered responses. *J Physiol*. 2011;589:2321-2348.
15. Osawa S, Weiss ER. A tale of two kinases in rods and cones. *Adv Exp Med Biol*. 2012;723:821-827.
16. Volff JN. Genome evolution and biodiversity in teleost fish. *Heredity (Edinb)*. 2005;94:280-294.
17. Saszik S, Bilotta J, Givin CM. ERG assessment of zebrafish retinal development. *Vis Neurosci*. 1999;16:881-888.
18. Bilotta J, Saszik S, Sutherland SE. Rod contributions to the electroretinogram of the dark-adapted developing zebrafish. *Dev Dyn*. 2001;222:564-570.
19. Lee BY, Thulin CD, Willardson BM. Site-specific phosphorylation of phosducin in intact retina. Dynamics of phosphorylation and effects on G protein beta gamma dimer binding. *J Biol Chem*. 2004;279:54008-54017.
20. Chrispell JD, Rebrik TI, Weiss ER. Electroretinogram analysis of the visual response in zebrafish larvae. *J Vis Exp*. 2015;97:52662.
21. Korenbrot JI, Mehta M, Tserentsoodol N, Postlethwait JH, Rebrik TI. EML1 (CNG-modulin) controls light sensitivity in darkness and under continuous illumination in zebrafish retinal cone photoreceptors. *J Neurosci*. 2013;33:17763-17776.
22. Kim DY, Jung CS. Gap junction contributions to the goldfish electroretinogram at the photopic illumination level. *Korean J Physiol Pharmacol*. 2012;16:219-224.
23. Cameron DJ, Rassamdana F, Tam P, et al. The optokinetic response as a quantitative measure of visual acuity in zebrafish. *J Vis Exp*. 2013;80:50832.
24. Naka KI, Rushton WA. S-potentials from colour units in the retina of fish (Cyprinidae). *J Physiol*. 1966;185:536-555.
25. Beltran WA, Allore HG, Johnson E, et al. CREB1/ATF1 activation in photoreceptor degeneration and protection. *Invest Ophthalmol Vis Sci*. 2009;50:5355-5363.
26. Otto-Bruc AE, Fariss RN, Van Hooser JP, Palczewski K. Phosphorylation of photolyzed rhodopsin is calcium-insensitive in retina permeabilized by alpha-toxin. *Proc Natl Acad Sci U S A*. 1998;95:15014-15019.
27. Ramamurthy V, Niemi GA, Reh TA, Hurley JB. Leber congenital amaurosis linked to AIPL1: a mouse model reveals destabilization of cGMP phosphodiesterase. *Proc Natl Acad Sci U S A*. 2004;101:13897-13902.
28. Branchek T. The development of photoreceptors in the zebrafish, *brachydanio rerio*. II. Function. *J Comp Neurol*. 1984;224:116-122.
29. Schmitt EA, Dowling JE. Early retinal development in the zebrafish, *Danio rerio*: light and electron microscopic analyses. *J Comp Neurol*. 1999;404:515-536.
30. Perlman I. The electroretinogram: ERG. In: Kolb H, Fernandez E, Nelson R, eds. *Webvision: The Organization of the Retina and Visual System*. Salt Lake City, UT: University of Utah Health Sciences Center; 1995. Available at: <https://webvision.med.utah.edu/book/electrophysiology/the-electroretinogram-erg/>.
31. Fleisch VC, Jametti T, Neuhauss SC. Electroretinogram (ERG) measurements in larval zebrafish. *CSH Protoc*. 2008;2008:pdb.prot4973.
32. Rinner O, Rick JM, Neuhauss SC. Contrast sensitivity, spatial and temporal tuning of the larval zebrafish optokinetic response. *Invest Ophthalmol Vis Sci*. 2005;46:137-142.
33. Postlethwait JH, Woods IG, Ngo-Hazelett P, et al. Zebrafish comparative genomics and the origins of vertebrate chromosomes. *Genome Res*. 2000;10:1890-1902.
34. Osawa S, Jo R, Weiss ER. Phosphorylation of GRK7 by PKA in cone photoreceptor cells is regulated by light. *J Neurochem*. 2008;107:1314-1324.
35. Kok FO, Shin M, Ni CW, et al. Reverse genetic screening reveals poor correlation between morpholino-induced and mutant phenotypes in zebrafish. *Dev Cell*. 2015;32:97-108.
36. Tachibanaki S, Shimauchi-Matsukawa Y, Arinobu D, Kawamura S. Molecular mechanisms characterizing cone photoreceptors. *Photochem Photobiol*. 2007;83:19-26.
37. Hamel CP. Cone rod dystrophies. *Orphanet J Rare Dis*. 2007;2:7.
38. Suzuki SC, Bleckert A, Williams PR, Takechi M, Kawamura S, Wong RO. Cone photoreceptor types in zebrafish are generated by symmetric terminal divisions of dedicated precursors. *Proc Natl Acad Sci U S A*. 2013;110:15109-15114.
39. Allison WT, Barthel LK, Skebo KM, Takechi M, Kawamura S, Raymond PA. Ontogeny of cone photoreceptor mosaics in zebrafish. *J Comp Neurol*. 2010;518:4182-4195.
40. Chen CK, Zhang K, Church-Kopish J, et al. Characterization of human GRK7 as a potential cone opsin kinase. *Mol Vis*. 2001;7:305-313.
41. Sears S, Erickson A, Hendrickson A. The spatial and temporal expression of outer segment proteins during development of Macaca monkey cones. *Invest Ophthalmol Vis Sci*. 2000;41:971-979.
42. Carr RER, Ripp H. Rhodopsin kinetics and rod adaptation in Oguchi's disease. *Invest Ophthalmol Vis Sci*. 1967;6:426-436.
43. Yamamoto S, Sippel KC, Berson EL, Dryja TP. Defects in the rhodopsin kinase gene in the Oguchi form of stationary night blindness. *Nat Genet*. 1997;15:175-178.
44. Chen CK, Burns ME, Spencer M, et al. Abnormal photoresponses and light-induced apoptosis in rods lacking rhodopsin kinase. *Proc Natl Acad Sci U S A*. 1999;96:3718-3722.
45. Cideciyan AV, Zhao X, Nielsen L, Khani SC, Jacobson SG, Palczewski K. Null mutation in the rhodopsin kinase gene slows recovery kinetics of rod and cone phototransduction in man. *Proc Natl Acad Sci U S A*. 1998;95:328-333.
46. Haider NB, Jacobson SG, Cideciyan AV, et al. Mutation of a nuclear receptor gene, NR2E3, causes enhanced S cone syndrome, a disorder of retinal cell fate. *Nat Genet*. 2000;24:127-131.
47. Milam AH, Rose L, Cideciyan AV, et al. The nuclear receptor NR2E3 plays a role in human retinal photoreceptor differentiation and degeneration. *Proc Natl Acad Sci U S A*. 2002;99:473-478.
48. Cideciyan AV, Jacobson SG, Gupta N, et al. Cone deactivation kinetics and GRK1/GRK7 expression in enhanced S cone syndrome caused by mutations in NR2E3. *Invest Ophthalmol Vis Sci*. 2003;44:1268-1274.